Global Change Biology
celebrating 20 years

Global Change Biology (2014) **20**, 1955–1967, doi: 10.1111/gcb.12567

Simultaneous improvement in productivity, water use, and albedo through crop structural modification

DARREN T. DREWRY[1,2], PRAVEEN KUMAR[3,4] and STEPHEN P. LONG[5,6]

[1]*Climate Physics Group, Jet Propulsion Laboratory, California Institute of Technology, m/s 233-300, Pasadena, CA 91109-8099, USA,* [2]*Joint Institute for Regional Earth System Science & Engineering, University of California Los Angeles, 607 Charles E Young Drive East, Young Hall, Room 4242, Los Angeles, CA 90095-7228, USA,* [3]*Department of Civil and Environmental Engineering, University of Illinois, 2527B Hydrosystems Laboratory, 301 North Mathews Avenue, Urbana, IL 61801-2352, USA,* [4]*Department of Atmospheric Sciences, University of Illinois, 150 South Gregory Street, Urbana, IL 61801-3070, USA,* [5]*Department of Crop Sciences, University of Illinois, AW-101 Turner Hall, 1102 South Goodwin Avenue, Urbana, IL 61801, USA,* [6]*Department of Plant Biology, University of Illinois, 265 Morrill Hall, 505 South Goodwin Avenue, Urbana, IL 61801, USA*

Abstract

Spanning 15% of the global ice-free terrestrial surface, agricultural lands provide an immense and near-term opportunity to address climate change, food, and water security challenges. Through the computationally informed breeding of canopy structural traits away from those of modern cultivars, we show that solutions exist that increase productivity and water use efficiency, while increasing land-surface reflectivity to offset greenhouse gas warming. Plants have evolved to maximize capture of radiation in the upper leaves, thus shading competitors. While important for survival in the wild, this is suboptimal in monoculture crop fields for maximizing productivity and other biogeophysical services. Crop progenitors evolved over the last 25 million years in an atmosphere with less than half the [CO_2] projected for 2050. By altering leaf photosynthetic rates, rising [CO_2] and temperature may also alter the optimal canopy form. Here using soybean, the world's most important protein crop, as an example we show by applying optimization routines to a micrometeorological leaf canopy model linked to a steady-state model of photosynthesis, that significant gains in production, water use, and reflectivity are possible with no additional demand on resources. By modifying total canopy leaf area, its vertical profile and angular distribution, and shortwave radiation reflectivity, all traits available in most major crop germplasm collections, increases in productivity (7%) are possible with no change in water use or albedo. Alternatively, improvements in water use (13%) or albedo (34%) can likewise be made with no loss of productivity, under Corn Belt climate conditions.

Keywords: agriculture, albedo, carbon uptake, climate change, crop breeding, crop ideotype, evapotranspiration, plant optimization, sustainability, water use efficiency

Received 21 August 2013 and accepted 24 October 2013

Introduction

Global demand for the major grain and seed crops is beginning to outstrip production for the first time in more than four decades, complicating decisions at the intersection of food security, water use, and climate change mitigation (Godfray *et al.*, 2010; Strzepek & Boehlert, 2010; Foley *et al.*, 2011). Trends in population growth and the expansion of the middle class globally have driven calls for a near doubling of food production by the middle of the century (United Nations, 2011). At the same time, the yield gains for the major food crops have stagnated (Duvick & Cassman, 1999; Cassman *et al.*, 2003; Ray *et al.*, 2012), and at present rates of improvement, this doubling will not be achieved (Long & Ort, 2010). This can be attributed to the fact that the approaches of the Green Revolution are nearing their biological limits. Radical new approaches may therefore be needed if the yield jumps required to avoid significant shortages are to be realized. Yield potential of crop germplasm was increased during the Green Revolution primarily by improving the proportion of the plant's biomass partitioned into the harvested product (harvest index, HI) and the amount of radiation captured over the growing season (interception efficiency, ε_i) (Long *et al.*, 2006a; Murchie *et al.*, 2009). However, with HI for elite modern crop germplasm now at approximately 60% (Evans, 1993; Hay, 1995) and ε_i at approximately 90% (Beadle & Long, 1985), these traits are close to their biological limits (Long *et al.*, 2006a). Crop photosynthesis, however, falls far short

Correspondence: Darren T. Drewry, tel. +818 393 2992, e-mail: ddrewry@jpl.nasa.gov; Praveen Kumar, tel. +217-333-4688, e-mail: kumar1@illinois.edu

of its theoretical maximum (Murchie *et al*., 2009; Zhu *et al*., 2010). Experimental open-air elevation of atmospheric CO_2 concentration [CO_2] around rice, soybean, and wheat crops in the field increases photosynthesis and in turn crop yields (Long *et al*., 2006b). We show here that by radical redesign of crop canopies, through conventional breeding, a large increase in photosynthetic carbon gain and in turn, yield potential could be achieved while improving or maintaining other ecosystem service benefits.

Demand for greater yield is further complicated by concurrent environmental demands on agricultural systems, in particular, improved water use efficiency (WUE) to allow improved yields without increasing water demand (Wallace, 2000; Howell, 2001; Condon *et al*., 2004). In addition, the broad geographical extent of agricultural lands planted with the major annual food crops (Monfreda *et al*., 2008; Ramankutty *et al*., 2008) provides a large scale opportunity to biogeophysically engineer a key climate warming offset, increased crop albedo, which would effectively cause surface cooling (Lenton & Vaughan, 2009; Ridgwell *et al*., 2009; Singarayer *et al*., 2009; Woodward *et al*., 2009). Given that new seed is sown annually, this is a global warming offset that could be rapidly implemented compared to other geophysical engineering options, providing it is not detrimental to maintaining or increasing yield.

The functional traits of modern agricultural species reflect many millions of years of preceding evolution which has selected for survival and fecundity of the individual, which will include traits in conflict with maximizing yield, the aim of modern agriculture (Loomis, 1993; Denison *et al*., 2003). Our previous work has shown radiation to be suboptimally distributed in modern soybean cultivars (Drewry *et al*., 2010a,b) as a function of observed foliage density and distribution (Dermody *et al*., 2006). Insights such as these have made canopy morphological traits such as leaf erectness key targets of breeding and genetic modification aimed at yield increases (Long *et al*., 2006a; Sakamoto *et al*., 2006). A number of other traits, such as leaf angle (Austin *et al*., 1976), glaucousness (Johnson *et al*., 1983; Holmes & Keiller, 2002), and leaf hair properties (Holmes & Keiller, 2002) have been shown to impact shortwave reflectivity, modifying canopy light distribution. However, exploring the implications of all possible permutations of these characteristics experimentally would be exhaustive in time and resources. Since the results are governed by well-defined biophysical principles, a more effective initial way forward is to use high performance computing to explore all permutations. In so doing, we can predict the quantitative biophysical properties to select for breeding the optimized ideotype for objectives of increased productivity, water use, and albedo.

Soybean, together with corn with which it is rotated over much of the US Corn Belt, arguably forms the largest single ecosystem type in the 48 contiguous US States. It is the second most important crop in the United States in terms of area planted and the fourth most important in terms of global production (FAOSTAT, 2012). While this investigation focuses on soybean, the principles developed would apply equally to the other major food crops.

The degree to which fundamental biophysical tradeoffs will limit the flexibility of agricultural systems to be managed to simultaneously improve crop yield, water use, and canopy reflectivity is a critical open question whose answer will guide the management of future agricultural systems. Here, we leverage advances in numerical optimization (Vrugt & Robinson, 2007) and in the biophysical and biochemical modeling of crop canopies (Drewry *et al*., 2010a,b) to address this question, with the aim of opening new avenues for future breeding programs targeting canopy-scale traits. We ask the question: by selection of canopy-scale characteristics, can a substantial improvement be achieved over existing canopies of elite germplasm?

Materials and methods

We examine numerically if crop canopies could be redesigned to simultaneously achieve: (i) maximization of CO_2 uptake (Max A_n); (ii) minimization of water use, or transpiration (Min T_r); and (iii) maximization of total shortwave albedo (Max α_s). We conducted optimization experiments to explore the extent to which each of the three selection criteria above could be improved without deterioration in the others, and the extent to which simultaneous improvement could be achieved. These cases have unique applications. For example, in a dry climate, the improvement of water use without compromising productivity and albedo may be the priority, whereas in a climate where radiation is limiting, maximizing A_n with no change in water use or albedo may be the ideal goal. To address these objectives, the following canopy traits were varied: total canopy leaf area (leaf area index, LAI), leaf area density as a function of height [LAD(z)], photosynthetically active radiation reflectivity [$PAR_r(z)$], near-infrared radiation reflectivity [$NIR_r(z)$], and leaf angle [$\gamma(z)$]. Details of the canopy model formulation, simulation setup, optimization algorithm, and canopy optimization experimental design are provided below.

Multi-layer canopy simulations

The optimizations of canopy structural traits were conducted using a biophysical canopy model (MLCan) that has been parameterized for a modern soybean cultivar

growing in the US Corn Belt (Drewry *et al*., 2010a) and validated with respect to canopy-scale CO_2, water, and energy exchange (Drewry *et al*., 2010a). This model is now publicly available (Le *et al*., 2012). The soybean model canopy in these experiments was discretized into 15 layers vertically, which allows for the within-canopy resolution of biochemical, ecophysiological, and physical states and fluxes. The 15 layer discretization has been shown to be sufficient to accurately capture canopy-atmosphere mass and energy exchange for both maize and soybean canopies (Drewry *et al*., 2010a). At each canopy level, a coupled system of equations was solved representing the limiting biochemical steps of steady-state photosynthesis (Farquhar *et al*., 1980; Farquhar & Sharkey, 1982), stomatal conductance (Ball & Berry, 1982), leaf energy balance (Nikolov, 1995), and leaf boundary layer conductance (Nikolov & Zeller, 2003). Shortwave radiation absorption, reflection, and transmission through the canopy were computed at each canopy layer using a Beer's Law relationship that incorporates vegetation clumping, separating leaves in direct sunlight from those in diffuse and shaded light (Campbell & Norman, 1998).

Photosynthetically active and near-infrared shortwave bands were considered separately as green foliage interacts differently with these two portions of the shortwave spectrum. The longwave radiation regime was resolved through the canopy as a function of absorption of downwelling radiation and emission in each layer using the Stefan-Boltzmann equation (Campbell & Norman, 1998). Within-canopy gradients of wind speed were calculated using the mean momentum equation (Poggi *et al*., 2004). Gradients of humidity, temperature, and CO_2 were computed using a temporally averaged conservation of mass equation and assuming negligible storage within the canopy airspace (Katul *et al*., 2004). The complete mathematical formulation of the MLCan model, including all parameters describing the species-specific physiological and physical characteristics of the soybean canopy, are provided in Drewry *et al*. (2010a) and the supplementary material of that article.

The model was run at hourly time steps. The environmental forcing variables used to drive the canopy model include top-of-canopy wind speed, air temperature, humidity, CO_2 concentration, and downward photosynthetically active, near-infrared, and thermal radiation fluxes. Each MLCan run was for a full diurnal period using the mean environmental forcing measured at the Bondville, Illinois Ameriflux site (http://ameriflux.ornl.gov/fullsiteinfo.php?sid=44) (located at 40.0062° North 88.2904° West, in central IL, USA) on 15 clear-sky days in July and August during the three study years for which MLCan was previously validated (2002, 2004, 2006) for soybean crop carbon dioxide, water, and energy fluxes (Drewry *et al*., 2010a) (see Fig. S1). This mean diurnal forcing is representative of the conditions when the canopy is fully closed and seed filling is occurring, and therefore a critical period in crop development. We focus on clear-sky conditions as these representative periods, in which the canopy is most likely to have high levels of both carbon dioxide assimilation and subsurface moisture utilization, making these periods the most challenging and critical for enhancing both productivity and moisture conservation.

Acclimatory response to climate change

Above-canopy CO_2 concentration was set to 370 ppm for the 'Current Climate' simulations, to represent the average value during the model validation years (2001–2006). Canopy simulations for the elevated CO_2 scenarios incorporated acclimatory responses of soybean plants to growth in a 550 ppm environment (Ainsworth & Long, 2005; Dermody *et al*., 2006; Ort *et al*., 2006) as observed at the SoyFACE Free Air Carbon Enrichment (FACE) experiment in central Illinois. For these experiments, total canopy leaf area was increased by 10% to represent observed structural acclimation of the soybean canopy (Dermody *et al*., 2006). To represent the observed photosynthetic down-regulation under 550 ppm growth conditions (Ainsworth *et al*., 2002; Bernacchi *et al*., 2005), the maximum carboxylation velocity of Rubisco (V_{cmax}) was reduced by 5%. Variations in stomatal regulation of gas exchange as a function of ambient [CO_2] are simulated dynamically through the coupling of the Ball-Berry model (Ball & Berry, 1982) of stomatal conductance, a widely utilized biochemical model of photosynthesis (Farquhar *et al*., 1980), and a model of the energy balance of a leaf (Nikolov, 1995). This is identical to the methodology employed by Drewry *et al*. (2010b) and validated with observations from the SoyFACE site.

Optimization algorithm

The canopy optimization experiments were conducted using the AMALGAM multi-objective optimization algorithm (Vrugt *et al*., 2003; Vrugt & Robinson, 2007). AMALGAM is a genetically adaptive multi-algorithm that combines multiple search algorithms to ensure reliable and efficient global optimization. For each two-objective optimization performed here, a population size of 200 members and 50 000 model evaluations was utilized. The three-objective optimization utilized a population size of 1000 members and 500 000 model evaluations. The objective function computations, along with the parameters varied in the optimization experiments and their ranges of variability are discussed below.

Canopy traits

The optimization algorithm converged to the optimal canopy structural values by varying up to five canopy characteristics, depending on the specific experiment being conducted. The LAI was one free parameter in the optimization experiments, and was allowed to vary within the range 3.0–7.5 ($m^2\ m^{-2}$). This range contains the observed mean value of 5.34 ($m^2\ m^{-2}$) for the period considered here (Dermody *et al*., 2006; Drewry *et al*., 2010a).

Four canopy-level traits were allowed to vary vertically throughout the canopy domain: (i) the vertical distribution of foliage, or leaf area density [LAD(z)]; (ii) mean leaf

angle [$\gamma(z)$]; (iii) reflectivity to photosynthetically active radiation [$PAR_r(z)$]; and (iv) reflectivity to near-infrared radiation [$NIR_r(z)$]. The vertical distribution of foliage, LAD(z), was varied according to a two-parameter distribution previously used to model crop canopy structure (Boedhram *et al*., 2001; Drewry *et al*., 2010b).

$$\mathrm{LAD}(z) = \frac{\mathrm{LAI}}{\mathrm{d}z}.\exp\left(-(z - z_{\mathrm{opt}})^2/\sigma^2\right) \quad (1)$$

z_{opt} and σ^2 were allowed to vary over the ranges [0.01–1.0] and [0.3–5.0]. These values respectively control the location of the vertical LAD(z) peak value and the dispersion of the distribution vertically. These specified ranges allowed for the optimization algorithm to search the space of canopy foliage distributions ranging from near-uniform to strongly concentrated in a few canopy layers. In the above equation, dz is the canopy grid spacing.

The two shortwave reflectivity distributions, $PAR_r(z)$ and $NIR_r(z)$, were allowed to vary vertically through the canopy as a function of the distribution of their respective leaf-level absorptivities (α_p and α_n), which were selected from the ranges [0.7–0.9] and [0.1–0.3], and allowed to vary linearly through the canopy.

$$\mathrm{PAR_r}(z) = \frac{1 - \sqrt{\alpha_p}}{1 + \sqrt{\alpha_p}} \quad (2)$$

$$\mathrm{NIR_r}(z) = \frac{1 - \sqrt{\alpha_n}}{1 + \sqrt{\alpha_n}} \quad (3)$$

Vertical variation in mean leaf angle was obtained by allowing a linearly varying profile of the leaf angle distribution parameter, x, bounded by values in the range [0–10] (Campbell, 1986), in the following equation that describes the extinction coefficient for beam radiation (K_b), which is also a function of the solar zenith angle (ϕ) (Drewry *et al*., 2010a).

$$K_b(z) = \frac{\sqrt{x^2 + \tan^2\phi}}{x + 1.774(x + 1.182)^{-0.733}} \quad (4)$$

The vertical distribution of mean leaf angle is calculated as the inverse cosine of $K_b(z)$ for a zenith angle of zero (Campbell, 1986):

$$\gamma(z) = \arccos\left[\frac{\sqrt{x^2}}{x + 1.774(x + 1.182)^{-0.733}}\right] \quad (5)$$

Model optimization experiments

Optimization experiments were conducted for two or three simultaneous goals, and by allowing one or a combination of several traits to vary together. This approach provided insight into the individual traits that produced the greatest benefit with respect to optimal goal values, and which trait combinations together provide the greatest, and potentially synergistic, improvements in performance. The values of the three selection criteria (Max A_n, Min T_r, and Max α_s), or goals, were determined by computing total canopy CO_2 uptake, transpiratory water use, and outgoing shortwave radiation at each iteration of the optimization algorithm. Total net canopy CO_2 uptake, A_n, which was maximized in the optimization experiments, was computed by vertically integrating through the plant canopy the net exchange of CO_2 uptake by all foliage, both sunlit and shaded, over the course of the diurnal period. The computation of total canopy water use, T_r, which was minimized in the optimization experiments, was similarly calculated by integrating vertically leaf water loss over all foliage over the diurnal period. No precipitation or dew accumulation was allowed on the foliage in these experiments to limit consideration to water use through transpiration. Total canopy shortwave albedo, α_s, which was maximized in the optimization experiments, was computed as the total upward photosynthetically active and near-infrared flux at the top of the canopy, also integrated over the diurnal period.

Optimization results are also presented in terms of WUE and radiation use efficiency (RUE). WUE is calculated as the ratio of daytime total CO_2 uptake over all foliage layers to daytime total water use by the canopy.

$$\mathrm{WUE} = \frac{\int_{t1}^{t2}\int_0^h A_{n,t}(z,t)\mathrm{d}z\mathrm{d}t}{\int_{t1}^{t2}\int_0^h T_{r,t}(z,t)\mathrm{d}z\mathrm{d}t} \quad (6)$$

RUE is calculated similarly, with the denominator representing the total daytime shortwave radiation absorbed by the canopy.

$$\mathrm{RUE} = \frac{\int_{t1}^{t2}\int_0^h A_{n,t}(z,t)\mathrm{d}z\mathrm{d}t}{\int_{t1}^{t2}\int_0^h \mathrm{SW}_{\mathrm{abs},t}(z,t)\mathrm{d}z\mathrm{d}t} \quad (7)$$

The variables $A_{n,t}(z, t)$, $T_{r,t}(z, t)$, and $SW_{abs,t}(z, t)$ represent, respectively, foliage CO_2 uptake, water use, and absorbed shortwave radiation at each canopy layer and model time step, h the height of the soybean canopy, and $t1$ and $t2$ the start and end times of the day.

Results

The canopy model optimization results are presented as changes in each objective (A_n, T_r, or α_s) produced by the new *in silico* optimized canopy, relative to the solution produced by a simulation with the 'control canopy', which is based on that measured for a current elite line in the field. The symbol Δ represents the percent change in a variable, as shown below for a hypothetical variable v.

$$\Delta v = \frac{v_{\text{optimized canopy}} - v_{\text{control canopy}}}{v_{\text{control canopy}}} \times 100\% \quad (8)$$

The control canopy was defined by the MLCan model description given in the Methods section above and elaborated in detail in Drewry *et al*. (2010a) and supporting information therein, including the parameter specifications provided for the measured soybean canopy. MLCan has been rigorously validated under current and future elevated CO_2 atmospheres (Drewry *et al*., 2010a,b). The optimization results are also presented in terms of water and radiation use efficiencies

(WUE and RUE, respectively), two metrics widely used in agricultural research to quantify resource utilization and potential limitations in crop production (Doorenbos *et al.*, 1979; Horton, 2000; Wallace, 2000).

Two-objective optimizations

The two panels of Fig. 1 show that with the redesign of the canopy, simultaneous and large improvements (gray quadrants) are possible in productivity and water use (Fig. 1a) and in productivity and albedo (Fig. 1b). The set of solutions for each combination of traits forms a convex set known as a Pareto Front, or optimality front, which shows the extent to which two or more objectives can be met simultaneously. Each optimality front contains the optimal solutions for each single objective, as end points. The other points on the optimality front present the range of possible trade-offs between two or more objectives. In Fig. 1a, the left-most colored square in the gray quadrant (orange circle '2') shows that an almost 13.5% reduction in water use is possible with no loss of productivity. Following this optimality front to the right through the quadrant, it may be seen that an almost 7% increase in productivity can be achieved with no additional water use (green circle '1').

In Fig. 1, the results from several two-objective optimization experiments are presented that demonstrate the extent to which one or more of the five canopy structural traits [LAI, LAD(z), $PAR_r(z)$, $NIR_r(z)$, $\gamma(z)$] can be modified individually or in combination to simultaneously improve two goals, [Max A_n, Min T_r] and [Max A_n, Max α_s]. Variations in either $PAR_r(z)$ or $NIR_r(z)$ are shown to have a negligible effect on A_n,

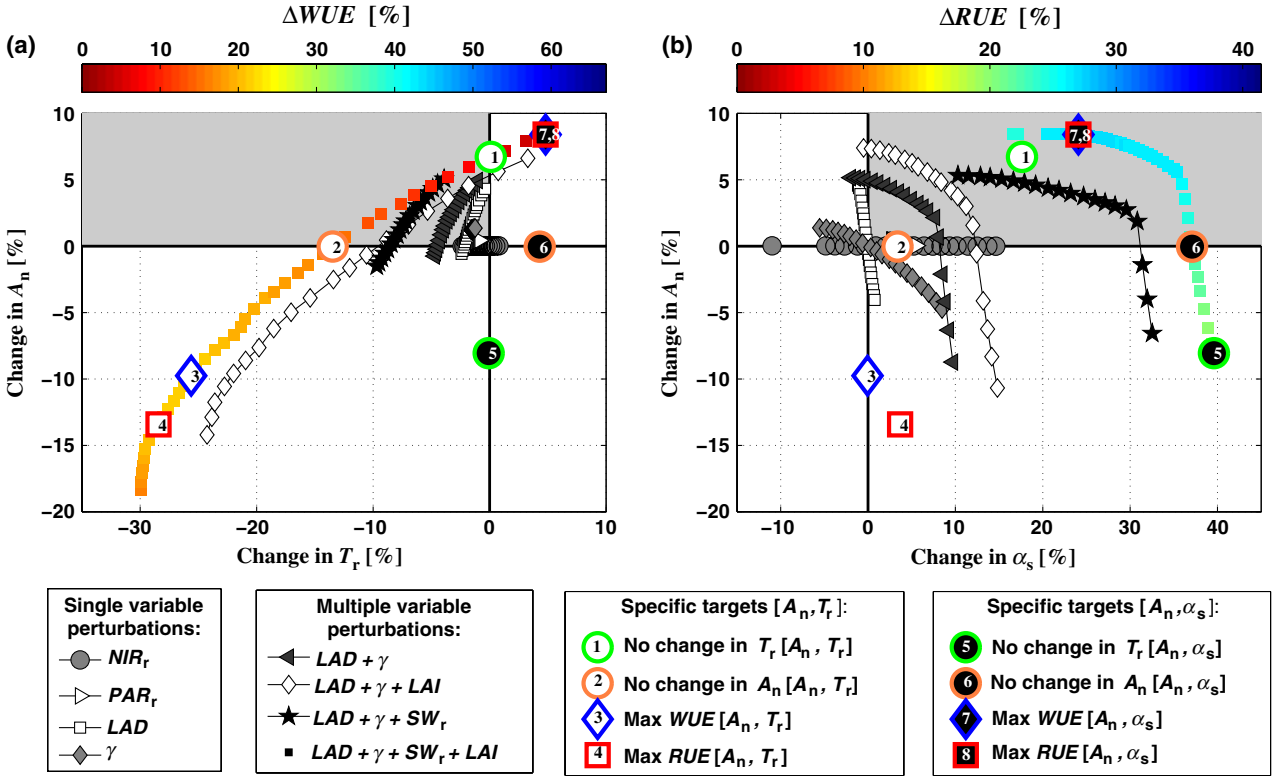

Fig. 1 Trade-offs in optimal improvements in productivity, water use (or transpiration), and albedo for present-day climate. The 2D optimality fronts representing trade-offs between increased canopy productivity (A_n) and reduced transpiration (T_r) are represented in panel (a), and those between increased A_n and increased canopy albedo (α_s) are presented in panel (b). Results are presented corresponding to optimization experiments, in which one or more of the canopy traits are allowed to vary. Portions of the fronts falling within the gray shaded quadrants represent solutions that produce improvements in both goals. Simultaneous achievement in both goals occurs for all but a few trait combinations. Solid colored squares correspond to the simultaneous variation in all traits examined in this study, with the symbol colors mapping to changes in water use efficiency (WUE; Panel a) and radiation use efficiency (RUE; Panel b) relative to the present observed (control) canopy. Example specific targets are indicated by large white-filled [(A_n,T_r) panel] and black-filled [(A_n,α_s) panel] symbols on the 'all-trait variation' fronts. Numbers on the symbols allow for comparison between specific targets. These include the maximization of resource use efficiencies and the solutions that maximize one objective while not negatively impacting the other objective.

indicating that the amount of shortwave radiation absorbed during the course of a cloud-free day is not constraining photosynthesis and that a canopy-scale bottleneck may exist in another aspect of the canopy structure. The single trait having the greatest impact on A_n is LAD(z), with the combined variation in [LAD(z), γ(z)] resulting in an almost 5% decrease in transpiration for no loss of productivity relative to the control canopy, or alternatively a 5% increase in productivity with a slight reduction in water use (Fig. 1a). Augmenting the variable set to include either LAI or both shortwave reflectivities [SW_r(z)], i.e. [LAD(z), γ(z), LAI] or [LAD(z), γ(z), PAR_r(z), NIR_r(z)], results in conservation of water, through reduced transpiration, of approximately 10% without loss of productivity (Fig. 1a).

Canopy albedo is most sensitive to variations in NIR reflectivity. PAR_r(z) or NIR_r(z) variations provide an opportunity for canopy shortwave albedo to be increased by up to 6% and 15%, respectively, with no cost to canopy productivity. Leaf angle distribution alone also has a large impact on canopy reflectance, increasing α_s by up to 8.5% (Fig. 1b). Variations in LAD(z) and γ(z) individually do not produce simultaneous improvement in A_n and α_s, but together synergistically provide a range of possible solutions that improve both goals at the same time (Fig. 1b, gray quadrant). Varying the reflectivities in combination with canopy foliage distribution and leaf angle variation [LAD(z), γ(z), PAR_r(z), NIR_r(z)] can produce a greater than 30% increase in total canopy albedo without loss of productivity (Fig. 1b).

When all traits are allowed to vary simultaneously [LAI, LAD(z), PAR_r(z), NIR_r(z), γ(z)], the optimality fronts in Fig. 1 describe solutions that improve WUE by as much as 21% for (A_n, T_r) and RUE by 27% for (A_n,α_s), as indicated by the coloring of the all-trait variation scenarios and associated color bars in Fig. 1a,b. It is of note that ideotypes related to 'specific target solutions' in one of the two-objective spaces, presented as large numbered symbols in Fig. 1, may perform poorly when the third objective is considered. For example, the solution that minimizes T_r while maintaining A_n at the control canopy level (Fig. 1a; orange circle '2') results in a small improvement in α_s (Fig. 1b), while the canopy that maximizes α_s for no relative change in A_n (Fig. 1b; symbol '6') results in increased canopy water use by more than 4% (Fig. 1a). Three of the four specific target solutions in the (A_n,α_s) objective space result in an increase in transpiration in the (A_n,T_r) space, with the only exception being the solution in which T_r is constrained to remain unchanged (symbol '5'). This contrasts with the (A_n,T_r) target solutions, which all show increases in shortwave reflectivity. These considerations demonstrate the power of this multi-objective optimization approach to guide solutions that simultaneously meet a range of agricultural goals. Overall, the two-objective optimization experiments show significant opportunities for simultaneous improvements in key agricultural goals.

Trait variations across optimality fronts

Figures 2 and 3 present the variations in structural traits across the optimality fronts when all traits are allowed to vary simultaneously (colored fronts in Fig. 1a,b). In Fig. 2, Panel (a) displays the variation in the three objectives and LAI for the all-trait optimality front in Fig. 1a, sorted with respect to ΔA_n. ΔA_n can be seen to increase monotonically, almost linearly, from left to right. ΔT_r also increases monotonically, nonlinearly rising as ΔA_n reaches its largest gains. Panels (b–d) in Fig. 2 show the within-canopy variations of leaf area density, mean leaf angle, and PAR reflectivity, sorted in the same manner with respect to ΔA_n. Vertical black dashed lines separate regions where a significant shift in the structure of the canopy occurs. Region 1 is comprised of the canopies with the greatest conservation of water. This occurs with a dense canopy near the surface that has horizontal and highly reflective foliage uniformly throughout the canopy space. The trade-off to reducing productivity losses (ΔA_n growing less negative) at the expense of water use begins in Region 2 as the foliage becomes less horizontally arrayed at the canopy top, allowing radiation to penetrate and excite photosynthesis in the lower-canopy foliage. These trends in ΔA_n and ΔT_r continue as canopy-top foliage becomes less reflective in the photosynthetically active portion of the spectrum, resulting in greater photosynthetic activity and transpiration. A further adjustment of the canopy-top foliage to more vertical orientation provides further productivity gains prior to entering Region 3, where a strong transition in leaf area density occurs, in which canopies with more uniform distributions continue to allow ΔA_n and ΔT_r to increase. The fluctuations of the structural traits in Region 3 illustrate the complex interactions between these variables that are required to produce a smooth optimality front that expresses the fundamental trade-offs between productivity and water use. Further increases in ΔA_n and ΔT_r are facilitated as LAI begins to increase from its lowest value in Region 4. As the canopies become denser, continued increases in LAI are coupled with a redistribution of the foliage in Region 5, allowing positive gains to be made in productivity relative to the control canopy. The canopies providing the largest gains in A_n have high values of PAR_r. This is due to the fact that for the reflectance model utilized here (Eqns 2 and 3), at high absorptivity values for PAR, transmission and reflectance covary

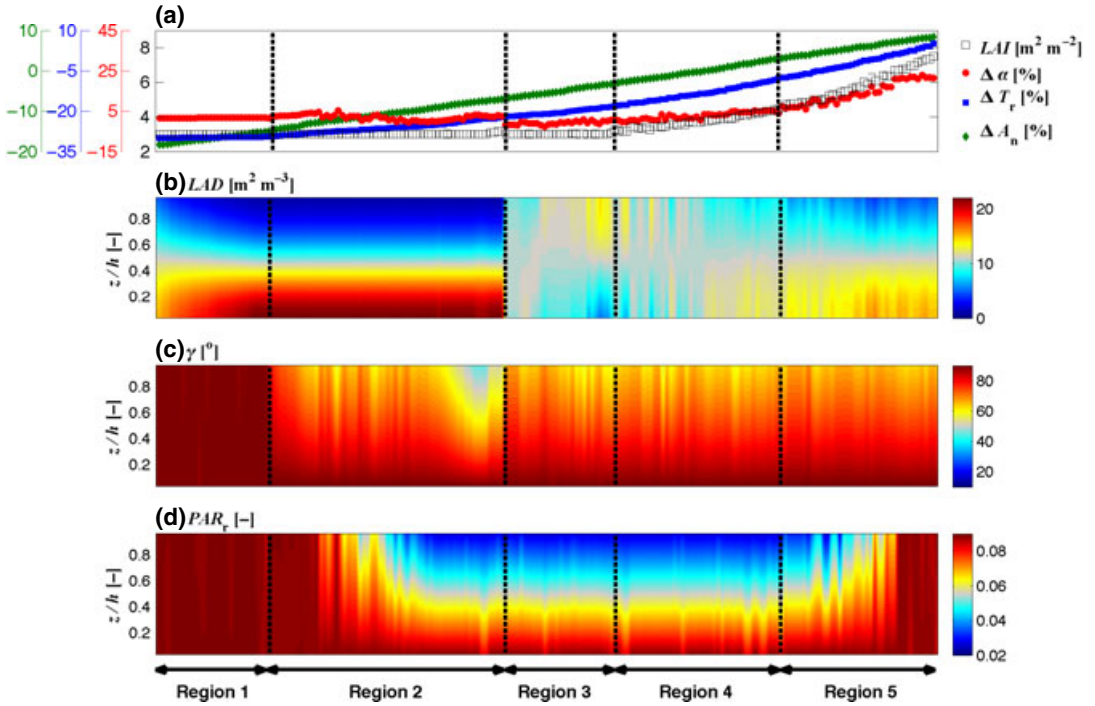

Fig. 2 Variation in structural traits for the (A_n,T_r) all-trait variation optimality front in Fig. 1a. Panel (a) shows the variation in the three objectives, and LAI, sorted by increasing ΔA_n. Panels (b–d) show the within-canopy variation in leaf area density, mean leaf angle, and PAR leaf reflectivity, respectively, also sorted by increasing ΔA_n. Vertical black dashed lines delineate major transitions in structural traits across the optimality front.

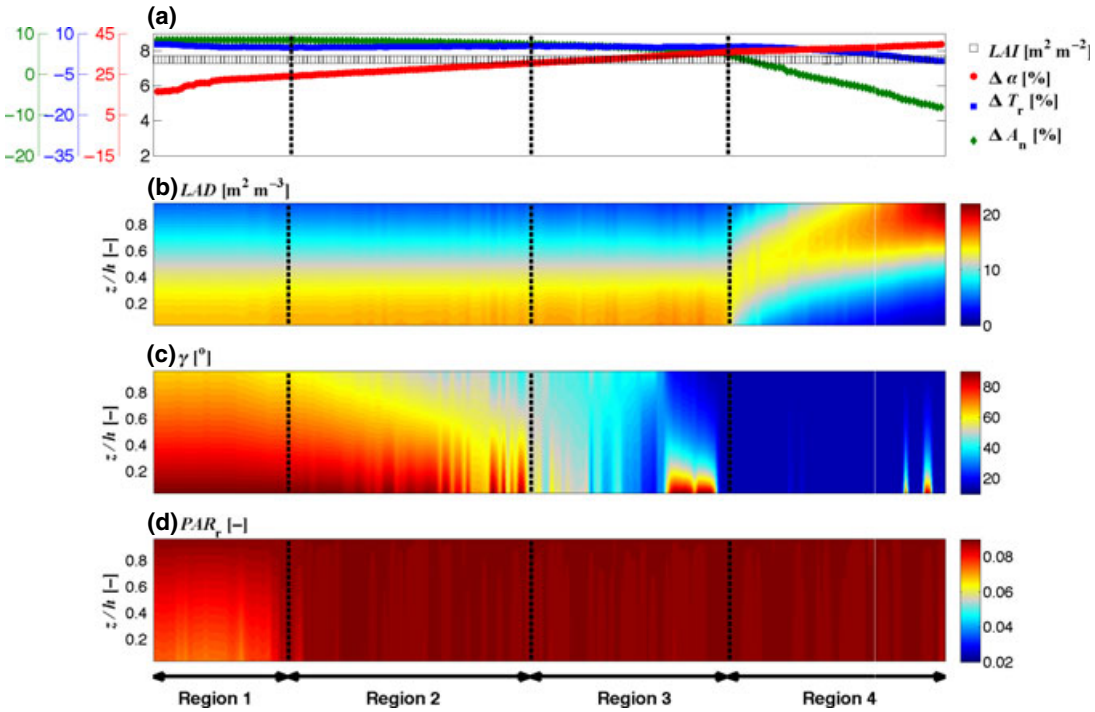

Fig. 3 Same as Fig. 2 for variation in structural traits for the (A_n, α_s) all-trait variation optimality front in Fig. 1b. Panel (a) shows the variation in the three objectives, and LAI, sorted by increasing ΔA_n. Panels (b–d) show the within-canopy variation in leaf area density, mean leaf angle, and PAR leaf reflectivity, respectively, also sorted by increasing ΔA_n. Vertical black dashed lines delineate major transitions in structural traits across the optimality front.

such that an increase in reflectance is accompanied by an increase in transmission. This increase in transmission, at the highest allowed LAI in these experiments (7.5 m^2 m^{-2}), allows greater photosynthesis deep in the canopy and thus provides a slight increase in A_n relative to higher absorptivity cases. NIR_r shows little variability for these solutions, varying between 0.50 and 0.52.

In Fig. 3, a similar set of panels describe the within-canopy trait variations as canopy albedo monotonically increases from left to right for the all-trait variation optimality front of Fig. 1b. For maximization of A_n and α_s, LAI remains at its maximum value of 7.5 m^2 m^{-2}. The highest A_n gains, and lowest α_s gains, are found in Region 1 with an LAD distribution that is more uniform than the control canopy, but with denser foliage near the surface, similar to that found for the highest ΔA_n canopies in the (A_n, T_r) space (Fig. 2). Leaves in Region 1 become more vertical and less reflective in the PAR regime with depth. In Region 2, albedo increases with little cost to A_n through simultaneous modifications to the leaf angle distribution that make canopy-top leaves more horizontal and PAR reflectivity increases with depth. These trends in A_n and α_s continue in Region 3 as the foliage throughout the canopy is made progressively more horizontal. It is notable that the changes across Regions 1–3 do not result in significant reductions in A_n, as the multi-objective optimization is able to find variations in LAD and PAR_r that offset the impacts of leaf angle variations, allowing gains in albedo to occur at almost no cost to productivity. A major shift in leaf area distribution occurs in Region 4, allowing albedo to continue to increase, but with a dramatic decline in productivity. As the foliage is made denser near the canopy top, leaves throughout the canopy are horizontally arrayed and have high PAR reflectance, producing the canopies with highest total albedo. NIR_r shows little variability for these solutions, varying between 0.47 and 0.52, allowing for maximum shortwave albedo by reflecting much of the radiation that is surplus to that needed to drive photosynthesis at light-saturation.

Elevated CO_2 impacts

Optimizations were repeated for increased [CO_2] to 550 ppm, relative to 370 ppm, and increases in air temperature (T_a) from 1 to 3 °C. Simultaneous variation in all traits were considered for these experiments (Fig. 4). As has been previously found by *in situ* measurement of the crop (Ainsworth & Long, 2005; Drewry *et al.*, 2010b), the C3 soybean plants demonstrate an increased photosynthetic capacity at 550 ppm. Here, this results in all of the optimality front solutions under climate change shifting to greater relative increases in A_n. The 370 ppm solutions are replotted in dashed boxes in Fig. 4 for comparison. Given the potential for rapid changes in climate and atmospheric composition over the coming decades, it is necessary to examine the extent to which the optimal ideotypes predicted from the model optimizations for current atmospheric conditions will provide similar improvements under anticipated conditions in coming decades. The exact canopy trait values that produced strong improvements in resource use efficiency under current climate (Fig. 1 numbered symbols) were simulated under the changing atmospheric conditions and projected onto the two-dimensional (2D) objective spaces in Fig. 4. Importantly, these current climate ideotypes do not deviate significantly from the optimality fronts that represent optimized plants for the climate change scenarios used, demonstrating the robust nature of these solutions. We note, however, that the specific target solutions found under current climate conditions often do not have their intended consequences, resulting, for example, in increased water use by up to 20% relative to target solutions designed specifically for the climate in which they are grown.

Three objective optimizations

A further optimization experiment was performed to determine if trait combinations exist that would simultaneously improve all three objectives (Fig. 5), through variation in all traits [LAD(z), γ(z), PAR_r(z), NIR_r(z), LAI]. The canopies found through multi-objective optimization show that a maximum improvement of productivity (6%), water use (13%), or albedo (34%) could be achieved with no detriment to the other objectives, with 16% of the solutions providing some level of improvement in all three goals simultaneously (solid color symbols on the three-dimensional (3D) surface, and dark symbols projected onto 2D planes in Fig. 5). As shown by the solutions in Fig. 5, the constraint that all three goals are met means that none of the goals achieve their maxima. Water use is decreased by as much as 30% when the other two goals are not considered. Looking at how WUE varies, relative to the control canopy, over the 3D surface (coloring and associated color bar in Fig. 5), for the solutions that maximize water conservation at the expense of both A_n and α_s (darker blue coloring), an increase in WUE is achieved through lower LAI values that allow greater radiation penetration and provide less foliage for transpiration. The green shaded portion of the surface in Fig. 5 corresponds to the region of the optimality front for which canopies have LAI values close to 5.34 (m^2 m^{-2}), the observed value from the empirical study

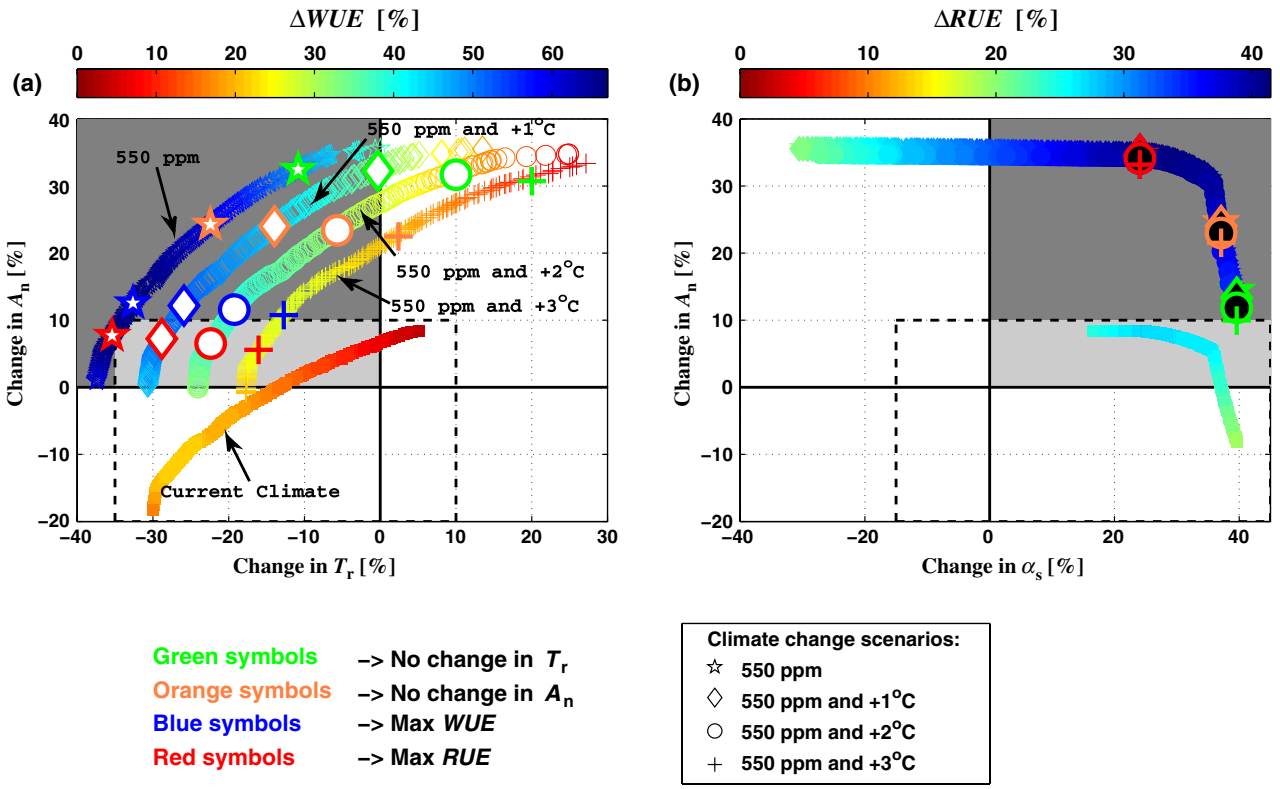

Fig. 4 Impact of rising temperature and atmospheric CO_2 on simultaneous improvements in productivity, water use, and albedo. 2D optimality fronts for the same objective pairs are as presented in Fig. 1. The dark gray regions depict the extension of the objective spaces in which improvement in both goals are made simultaneously, relative to the region displayed in Fig. 1. The dashed boxes contain the full extent of the axes in Fig. 1, along with the optimality fronts corresponding to the simultaneous variation in all traits under current climate conditions, for reference. The optimality fronts derived from optimizations for four climate change scenarios are presented. The symbols depicting each optimality front show changes in WUE (Panel a) and RUE (Panel b) relative to the control simulation for present temperature and [CO_2]. The canopy structures corresponding to the ideotypes depicted in Fig. 1 were also simulated for each climate change scenario and are plotted as large white- (Panel a) and black-filled (Panel b) symbols. The ideotypes derived from optimization to current temperature and [CO_2] fall very close to the climate change scenario optimality fronts examined here.

on which the present model was parameterized (Dermody *et al.*, 2006). Many of these solutions fall within the set of points that improve all objectives simultaneously, while some of them improve α_s at the expense of Max A_n, as maximum α_s is achieved by leaf angle distributions that are nearly parallel to the surface. These results suggest a wide range of potential solutions to meet the specific goals for a given environment.

Optimal canopy profiles

The distributions of foliage and leaf angles for the canopies that maximize A_n, WUE, and α_s demonstrate a wide range of variability and significant differences with the control canopy. In Fig. 6, the top panels present the diurnal, canopy-resolved A_n for the Max A_n canopy (Panel a), T_r for the canopy that maximizes WUE (Panel b), and absorbed PAR for the canopy that maximizes albedo (Panel c). In each of these panels, contours provide the diurnal, canopy-resolved values of these variables for the control canopy. The canopy LAI profile overlaid on these plots shows the impact of the dense canopy-top foliage on CO_2 uptake, water exchange, and PAR absorption for the control canopy. The bottom panels show the difference between the specific target solutions and the control canopy diurnally through the canopy space, with the LAI profiles and mean leaf angles of each layer for the target solution canopies overlaid.

Maximization of WUE requires a thinner canopy [LAI = 3 (m^2 m^{-2})] (Fig. 6b,e), with 78% of the canopy foliage at less than half of the canopy height ($z/h < 0.5$), where h is the height of the canopy top. By transferring the majority of the leaf area down into a more sheltered environment near the surface, lower wind speeds, and higher humidity further reduce the transpiration of a canopy with significantly less surface

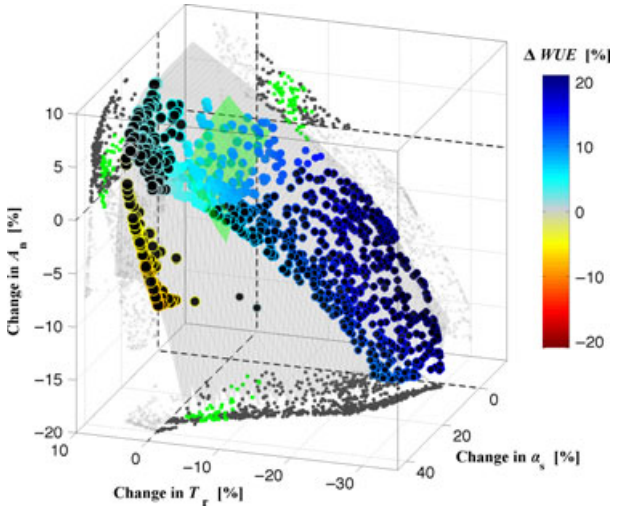

Fig. 5 Three-dimensional optimality front for productivity, water use, and albedo. Solid colored symbols indicate the canopies that simultaneously improve each of the three objectives, as opposed to black-filled symbols that represent improvement in only one or two objectives. Projections onto each 2D plane indicate those canopies that meet all three objectives (black dots) and those which do not (light gray symbols). The green region of the optimality front spans the canopies whose densities lie in the range $5.0 \leq \text{LAI} \leq 5.7$ ($m^2\ m^{-2}$), close to the observed canopy density of 5.34 ($m^2\ m^{-2}$). On the 3D optimality front symbol size is proportional to LAI value, ranging from 3.0 to 7.5 ($m^2\ m^{-2}$).

area for transpiration. This form of canopy redesign contrasts sharply with the optimal ideotype to maximize A_n (Fig. 6a,d) and α_s (Fig. 6c,f), both of which are characterized by the densest allowed foliage in these experiments [LAI = 7.5 ($m^2\ m^{-2}$)]. The canopy that maximizes A_n has a more uniform LAD profile, with 60% of the foliage at $z/h < 0.5$, resulting in a more uniform CO_2 uptake throughout the day relative to the control canopy. This foliage distribution acts to effectively maximize PAR utilization by maintaining sufficient PAR flux on canopy-top foliage, with higher photosynthetic capacities, but allowing excess radiation to penetrate to deeper canopy layers and excite photosynthesis more uniformly throughout the entire depth of the canopy. The impact of this is illustrated in the diurnal differences through the canopy in A_n and T_r between the Max A_n and Max WUE ideotypes and the control canopy (Fig. 6d,e). In these cases, significant reductions in A_n and T_r occur in the upper-canopy space for the ideotypes relative to the control canopy, which has an LAD maximum at approximately $z/h = 0.8$ (Fig. 6a,b). The losses in upper-canopy net CO_2 uptake shown in Fig. 6a, where foliage in the control canopy was light saturated at the expense of the shaded lower canopy (Drewry *et al.*, 2010a), are more than offset by increased photosynthetic assimilation in the denser lower canopy of the Max A_n ideotype (Fig. 6d).

The canopy that maximizes reflected shortwave radiation has a foliage distribution biased toward the upper canopy, with 84% of the foliage above the midpoint of the canopy. The leaves of this canopy are arrayed nearly parallel to the ground surface throughout the canopy. This structure results in greater absorbed PAR in a thin region of the upper canopy, but a 40% increase in total shortwave reflected back to the atmosphere, and reductions in absorbed PAR throughout approximately 90% of the canopy space. The influences of each of these ideotype canopy structures on A_n, T_r, and α_s throughout the canopy space are presented in Figs S2–S4.

Discussion

Our previous work has shown that the structural traits of modern soybean cultivars are suboptimal for productivity (Drewry *et al.*, 2010a,b). Previous efforts have demonstrated a correlation between canopy traits influencing photosynthesis and the light environment of the canopy for both natural and agricultural systems (e.g. Field, 1983; Field & Mooney, 1983; Hirose & Werger, 1987a; Chen *et al.*, 1993; Ellsworth & Reich, 1993; Hollinger, 1996; Posada *et al.*, 2009). Examinations of canopy optimality theory have also found discrepancies between the theoretically optimal set of traits describing canopy form and photosynthetic capacity and those observed (Hirose & Werger, 1987b), particularly when a broader set of traits, plant stresses, and environmental factors are included (Hollinger, 1996; Niinemets, 2007; Buckley *et al.*, 2013). Recent work examining canopy optimization theory in the context of heterogeneous systems has demonstrated the importance of considering the influence of neighboring plants on the light environment. Competition for light results in taller plants that distribute more leaf area horizontally (Anten, 2005). The necessity to maximize the capture of radiation in the upper leaves to shade competitors may confer advantages in the wild, but results in the evolution of suboptimal monoculture crop plants for maximizing productivity and other biogeophysical services.

The experiments presented here demonstrate that through the computationally informed breeding of canopy structural traits away from those of modern cultivars, significant gains in productivity, water use, and albedo can all be achieved. This assumes that genetic traits are likely to be available in major crop germplasm collections or transgenes are available to achieve these changes. Mutants for leaf erectness have been identified

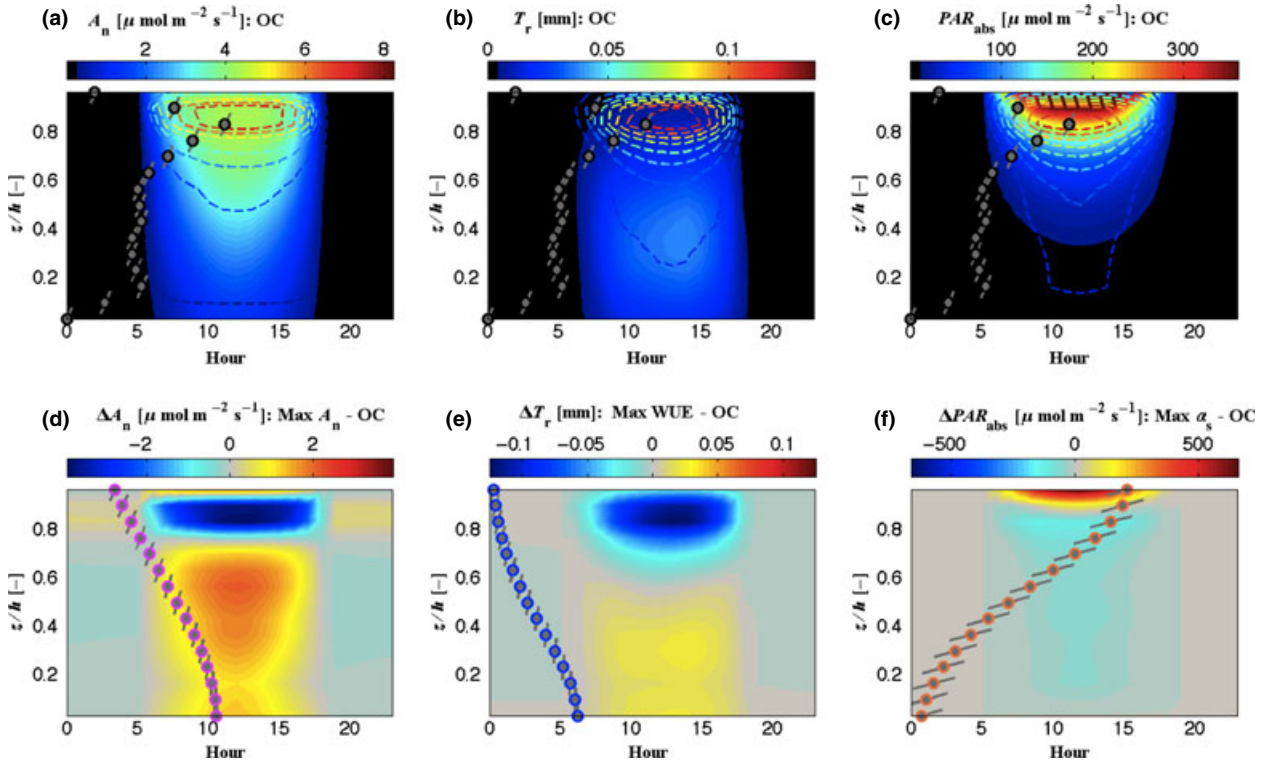

Fig. 6 Impact of optimal traits on canopy function and environment. Vertically resolved (within canopy) diurnal variations of A_n for the Max A_n canopy (Panel a), T_r for the canopy that maximizes WUE (Panel b), and absorbed PAR for the canopy that maximizes albedo (Panel c). In each of these panels, contours provide the diurnal, canopy-resolved values of these variables for the control canopy (OC). The observed leaf area density profile is presented as gray symbols, with lines through the symbols denoting the mean leaf angle of each canopy layer. The vertically resolved changes (optimal – control canopy variable) that result from optimal ideotypes representing notable solutions are presented in the bottom row. (d) The change net CO_2 assimilation that results from the maximization of A_n, (e) the change in transpiration that results from maximization of WUE and (f) the change in absorbed PAR that results from maximization of albedo. The LAD profiles and leaf angle profiles corresponding to these ideotypes are presented on each color plot.

for crops, including rice (Sakamoto *et al*., 2006; Zhao *et al*., 2010) and wheat (Tanner *et al*., 1966; De Carvalho & Qualset, 1978), and have been shown to significantly increase yield when plant spacing is also considered. Structural modification has been applied to increasing yields in both wheat and rice through the so-called 'Green Revolution genes', which introduced dwarfing traits that provided resistance to lodging and improved HI (Peng *et al*., 1999; Hedden, 2003). Changes in stature have a secondary effect of modifying leaf arrangement (Donald, 1968), and so could provide a path to modification in leaf area density to further improve yield. Genetic maps are being developed for soybean structural traits such as plant height, and leaf traits including area, width, and height (Mansur *et al*., 1996), which could allow canopy leaf area to be modified. Genes for leaf glaucousness have been identified for wheat (Watanabe *et al*., 2005) and have been shown to impact plant functional variables such as WUE, gas exchange, and leaf temperatures (Richards *et al*., 1986). Likewise, chlorophyll mutants could provide a basis for the modification of leaf-level radiation interactions in the PAR range (Buttery & Buzzell, 1977). Genetic approaches to improving plant water use and leaf gas exchange properties are now being developed (Masle *et al*., 2005; Dodd *et al*., 2011), and in combination with synergistic structural modifications could provide a powerful new approach to extending yield gains.

Traditional crop improvement relies on crossing parents that may introduce single, required traits into elite lines followed by visual selection. With the slow generation time of crop plants, no more than two to three generations per year, decades can be required before improved germplasm is available. The current generation of biophysical vegetation models and numerical optimization techniques now opens the door for quickly identifying the range and combination of plant traits, which as seen here are nonintuitive and novel yet meet these needs. This study demonstrates a new way forward to address food security, diminished water resources, and climate change amelioration, three of the most pressing of the developing global issues.

Acknowledgements

This study was initiated under NSF Grant ATM 06-28687 when the first author was at the University of Illinois. This support is gratefully acknowledged. DTD further acknowledges support by the National Science Foundation International Research Fellowship Program (IRFP), award OISE-0900556. DTD also acknowledges support of the Jet Propulsion Laboratory, California Institute of Technology, under a contract with the National Aeronautics and Space Administration. SPL and PK acknowledge support from the Bill and Melinda Gates Foundation (OPP1060461) titled 'RIPE – Realizing Increased Photosynthetic Efficiency for Sustainable Increases in Crop Yield'. PK also acknowledges NSF awards CBET 12-09402 and EAR 13-31906, as well as support from the Civil and Environmental Engineering Department, University of Illinois, to support research on Water Security and Emergent Risks.

References

Ainsworth EA, Long SP (2005) What have we learned from 15 years of free-air CO_2 enrichment (FACE)? A meta-analytic review of the responses of photosynthesis, canopy properties and plant production to rising CO_2. *New Phytologist*, **165**, 351–372.

Ainsworth EA, Davey PA, Bernacchi CJ *et al.* (2002) A meta-analysis of elevated [CO_2] effects on soybean (glycine max) physiology, growth and yield. *Global Change Biology*, **8**, 695–709.

Anten NP (2005) Optimal photosynthetic characteristics of individual plants in vegetation stands and implications for species coexistence. *Annals of Botany*, **95**, 495–506.

Austin R, Ford M, Edrich J, Hooper B (1976) Some effects of leaf posture on photosynthesis and yield in wheat. *Annals of Applied Biology*, **83**, 1975.

Ball J, Berry J (1982) The Ci/Cs ratio: a basis for predicting stomatal control of photosynthesis. *Carnegie Institute of Washington Yearbook*, **81**, 88–92.

Beadle C, Long S (1985) Photosynthesis—is it limiting to biomass production? *Biomass*, **8**, 119–168.

Bernacchi CJ, Morgan PB, Ort DR, Long SP (2005) The growth of soybean under free air [CO_2] enrichment (FACE) stimulates photosynthesis while decreasing in vivo Rubisco capacity. *Planta*, **220**, 434–446.

Boedhram N, Arkebauer TJ, Batchelor WD (2001) Season-long characterization of vertical distribution of leaf area in corn. *Agronomy Journal*, **93**, 1235–1242.

Buckley TN, Cescatti A, Farquhar GD (2013) What does optimization theory actually predict about crown profiles of photosynthetic capacity when models incorporate greater realism? *Plant, Cell & Environment*, **36**, 1547–1563.

Buttery B, Buzzell R (1977) The relationship between chlorophyll content and rate of photosynthesis in soybeans. *Canadian Journal of Plant Science*, **57**, 1–5.

Campbell G (1986) Extinction coefficients for radiation in plant canopies calculated using an ellipsoidal inclination angle distribution. *Agricultural and Forest Meteorology*, **36**, 317–321.

Campbell GS, Norman JM (1998) *An Introduction to Environmental Biophysics*. Springer, New York.

Cassman KG, Dobermann A, Walters DT, Yang H (2003) Meeting cereal demand while protecting natural resources and improving environmental quality. *Annual Review of Environment and Resources*, **28**, 315–358.

Chen J-L, Reynolds JF, Harley PC, Tenhunen JD (1993) Coordination theory of leaf nitrogen distribution in a canopy. *Oecologia*, **93**, 63–69.

Condon AG, Richards RA, Rebetzke GJ, Farquhar GD (2004) Breeding for high water-use efficiency. *Journal of Experimental Botany*, **55**, 2447–2460.

De Carvalho FI, Qualset C (1978) Genetic variation for canopy architecture and its use in wheat breeding. *Crop Science*, **18**, 561–567.

Denison RF, Kiers ET, West SA (2003) Darwinian agriculture: when can humans find solutions beyond the reach of natural selection? *The Quarterly Review of Biology*, **78**, 145–168.

Dermody O, Long SP, DeLucia EH (2006) How does elevated CO_2 or ozone affect the leaf-area index of soybean when applied independently? *New Phytologist*, **169**, 145–155.

Dodd IC, Whalley WR, Ober ES, Parry MAJ (2011) Genetic and management approaches to boost UK wheat yields by ameliorating water deficits. *Journal of Experimental Botany*, **62**, 5241–5248.

Donald CM (1968) The breeding of crop ideotypes. *Euphytica*, **17**, 385–403.

Doorenbos J, Kassam AH *et al.* (1979) *Yield Response to Water*. Food and Agriculture Organization of the United Nations, Rome, Italy.

Drewry DT, Kumar P, Long S, Bernacchi C, Liang X-Z, Sivapalan M(2010a) Ecohydrological responses of dense canopies to environmental variability: 1. Interplay between vertical structure and photosynthetic pathway. *Journal of Geophysical Research*, **115**, G04022.

Drewry DT, Kumar P, Long S, Bernacchi C, Liang X-Z, Sivapalan M (2010b) Ecohydrological responses of dense canopies to environmental variability: 2. Role of acclimation under elevated CO_2. *Journal of Geophysical Research*, **115**, G04023.

Duvick D, Cassman KG (1999) Post–green revolution trends in yield potential of temperate maize in the North-Central United States. *Crop Science*, **39**, 1622–1630.

Ellsworth D, Reich P (1993) Canopy structure and vertical patterns of photosynthesis and related leaf traits in a deciduous forest. *Oecologia*, **96**, 169–178.

Evans LT (1993) *Crop Evolution, Adaptation and Yield*. Cambridge University Press, Cambridge, England.

FAOSTAT (2012) *FAO Statistical Databases*. Food and Agriculture Organization of the United Nations, Rome, Italy. http://www.fao.org.

Farquhar GD, Sharkey TD (1982) Stomatal conductance and photosynthesis. *Annual Review of Plant Physiology*, **33**, 317–345.

Farquhar G, von Caemmerer S, von Berry J (1980) A biochemical model of photosynthetic CO_2 assimilation in leaves of C3 species. *Planta*, **149**, 78–90.

Field C (1983) Allocating leaf nitrogen for the maximization of carbon gain: leaf age as a control on the allocation program. *Oecologia*, **56**, 341–347.

Field C, Mooney H (1983) Leaf age and seasonal effects on light, water, and nitrogen use efficiency in a California shrub. *Oecologia*, **56**, 348–355.

Foley JA, Ramankutty N, Brauman KA *et al.* (2011) Solutions for a cultivated planet. *Nature*, **478**, 337–342.

Godfray HCJ, Beddington JR, Crute IR *et al.* (2010) Food security: the challenge of feeding 9 billion people. *Science*, **327**, 812–818.

Hay R (1995) Harvest index: a review of its use in plant breeding and crop physiology. *Annals of Applied Biology*, **126**, 197–216.

Hedden P (2003) The genes of the Green Revolution. *Trends in Genetics*, **19**, 5–9.

Hirose T, Werger MJ (1987a) Nitrogen use efficiency in instantaneous and daily photosynthesis of leaves in the canopy of a Solidago altissima stand. *Physiologia Plantarum*, **70**, 215–222.

Hirose T, Werger M (1987b) Maximizing daily canopy photosynthesis with respect to the leaf nitrogen allocation pattern in the canopy. *Oecologia*, **72**, 520–526.

Hollinger D (1996) Optimality and nitrogen allocation in a tree canopy. *Tree Physiology*, **16**, 627–634.

Holmes M, Keiller D (2002) Effects of pubescence and waxes on the reflectance of leaves in the ultraviolet and photosynthetic wavebands: a comparison of a range of species. *Plant, Cell & Environment*, **25**, 85–93.

Horton P (2000) Prospects for crop improvement through the genetic manipulation of photosynthesis: morphological and biochemical aspects of light capture. *Journal of Experimental Botany*, **51**, 475–485.

Howell TA (2001) Enhancing water use efficiency in irrigated agriculture. *Agronomy Journal*, **93**, 281–289.

Johnson DA, Richards RA, Turner NC (1983) Yield, water relations, gas exchange, and surface reflectances of near-isogenic wheat lines differing in glaucousness. *Crop Science*, **23**, 318–325.

Katul GG, Mahrt L, Poggi D, Sanz C (2004) One- and two-equation models for canopy turbulence. *Boundary-Layer Meteorology*, **113**, 81–109.

Le PVV, Kumar P, Drewry DT, Quijano JC (2012) A graphical user interface for numerical modeling of acclimation responses of vegetation to climate change. *Computers & Geosciences*, **49**, 91–101.

Lenton TM, Vaughan NE (2009) The radiative forcing potential of different climate geoengineering options. *Atmospheric Chemistry and Physics*, **9**, 5539–5561.

Long SP, Ort DR (2010) More than taking the heat: crops and global change. *Current Opinion in Plant Biology*, **13**, 240–247.

Long SP, Naidu S, Ort D (2006a) Can improvement in photosynthesis increase crop yields? *Plant Cell and Environment*, **29**, 315–330.

Long SP, Ainsworth EA, Leakey ADB, Nösberger J, Ort DR (2006b) Food for thought: lower-than-expected crop yield stimulation with rising CO_2 concentrations. *Science*, **312**, 1918–1921.

Loomis R (1993) Optimization theory and crop improvement. *International Crop Science*, **I**, 583–588.

Mansur L, Orf J, Chase K, Jarvik T, Cregan P, Lark K (1996) Genetic mapping of agronomic traits using recombinant inbred lines of soybean. *Crop Science*, **36**, 1327–1336.

Masle J, Gilmore SR, Farquhar GD (2005) The ERECTA gene regulates plant transpiration efficiency in Arabidopsis. *Nature*, **436**, 866–870.

Monfreda C, Ramankutty N, Foley JA (2008) Farming the planet: 2. Geographic distribution of crop areas, yields, physiological types, and net primary production in the year 2000. *Global Biogeochemical Cycles*, **22**, 1–19.

Murchie E, Pinto M, Horton P (2009) Agriculture and the new challenges for photosynthesis research. *New Phytologist*, **181**, 532–552.

Niinemets U (2007) Photosynthesis and resource distribution through plant canopies. *Plant, Cell & Environment*, **30**, 1052–1071.

Nikolov N (1995) Coupling biochemical and biophysical processes at the leaf level: an equilibrium photosynthesis model for leaves of C3 plants. *Ecological Modelling*, **80**, 205–235.

Nikolov N, Zeller KF (2003) Modeling coupled interactions of carbon, water, and ozone exchange between terrestrial ecosystems and the atmosphere. I: Model description. *Environmental Pollution*, **124**, 231–246.

Ort DR, Ainsworth EA, Aldea M *et al*. (2006) SoyFACE: the effects and interactions of elevated CO_2 and O3 on soybean. In: *Managed Ecosystems and CO_2*, Vol. **187** (eds Nösberger J, Long SP, Norby RJ, Stitt M, Hendrey GR, Blum H, Caldwell MM, Heldmaier G, Jackson RB, Lange OL, Mooney HA, Schulze E-D, Sommer U), pp. 71–86. Springer, Berlin Heidelberg.

Peng J, Richards DE, Hartley NM *et al*. (1999) "Green revolution"genes encode mutant gibberellin response modulators. *Nature*, **400**, 256–261.

Poggi D, Porporato A, Ridolfi L, Albertson JD, Katul GG (2004) The effect of vegetation density on canopy sub-layer turbulence. *Boundary-Layer Meteorology*, **111**, 565–587.

Posada JM, Lechowicz MJ, Kitajima K (2009) Optimal photosynthetic use of light by tropical tree crowns achieved by adjustment of individual leaf angles and nitrogen content. *Annals of Botany*, **103**, 795–805.

Ramankutty N, Evan AT, Monfreda C, Foley JA (2008) Farming the planet: 1. Geographic distribution of global agricultural lands in the year 2000. *Global Biogeochemical Cycles*, **22**, GB1003.

Ray DK, Ramankutty N, Mueller ND, West PC, Foley JA (2012) Recent patterns of crop yield growth and stagnation. *Nature Communications*, **3**, 1293.

Richards R, Rawson H, Johnson D (1986) Glaucousness in wheat: its development and effect on water-use efficiency, gas exchange and photosynthetic tissue temperatures. *Functional Plant Biology*, **13**, 465–473.

Ridgwell A, Singarayer JS, Hetherington AM, Valdes PJ (2009) Tackling regional climate change by leaf albedo bio-geoengineering. *Current Biology*, **19**, 146–150.

Sakamoto T, Morinaka Y, Ohnishi T *et al*. (2006) Erect leaves caused by brassinosteroid deficiency increase biomass production and grain yield in rice. *Nature Biotechnology*, **24**, 105–109.

Singarayer JS, Ridgwell A, Irvine P (2009) Assessing the benefits of crop albedo bio-geoengineering. *Environmental Research Letters*, **4**, 045110.

Strzepek K, Boehlert B (2010) Competition for water for the food system. *Philosophical Transactions of the Royal Society B: Biological Sciences*, **365**, 2927–2940.

Tanner J, Gardener C, Stoskopf N, Reinbergs K (1966) Some observations on upright-leaf-type small grains. *Canadian Journal of Plant Science*, **46**, 690–690.

United Nations (2011) *The Great Green Technological Transformation*. United Nations, New York.

Vrugt JA, Robinson BA (2007) Improved evolutionary optimization from genetically adaptive multimethod search. *Proceedings of the National Academy of Sciences*, **104**, 708–711.

Vrugt JA, Gupta HV, Bastidas LA, Bouten W, Sorooshian S (2003) Effective and efficient algorithm for multiobjective optimization of hydrologic models. *Water Resources Research*, **39**, 1214.

Wallace JS (2000) Increasing agricultural water use efficiency to meet future food production. *Agriculture, Ecosystems & Environment*, **82**, 105–119.

Watanabe N, Takesada N, Shibata Y, Ban T (2005) Genetic mapping of the genes for glaucous leaf and tough rachis in Aegilops tauschii, the D-genome progenitor of wheat. *Euphytica*, **144**, 119–123.

Woodward FI, Bardgett RD, Raven JA, Hetherington AM (2009) Biological approaches to global environment change mitigation and remediation. *Current Biology*, **19**, R615–R623.

Zhao S-Q, Hu J, Guo L-B, Qian Q, Xue H-W (2010) Rice leaf inclination2, a VIN3-like protein, regulates leaf angle through modulating cell division of the collar. *Cell Research*, **20**, 935–947.

Zhu X-G, Long SP, Ort DR (2010) Improving photosynthetic efficiency for greater yield. *Annual Review of Plant Biology*, **61**, 235–261.

Supporting Information

Additional Supporting Information may be found in the online version of this article:

Figure S1 Environmental forcing variables at top of canopy used to conduct simulations.
Figure S2 Impact of specific target goals on canopy structures and net canopy CO_2 uptake (A_n).
Figure S3 Impact of specific target goals on canopy structures and canopy transpiration (T_r).
Figure S4 Impact of specific target goals on canopy structures and absorbed canopy photosynthetically active radiation flux (PAR_{abs}).